

AmbiMax: Autonomous Energy Harvesting Platform for Multi-Supply Wireless Sensor Nodes

Chulsung Park and Pai H. Chou

Center for Embedded Computer Systems, University of California, Irvine, CA 92697-2625 USA

Email: {chulsung, phchou}@uci.edu

Abstract—AmbiMax is an energy harvesting circuit and a supercapacitor based energy storage system for wireless sensor nodes (WSN). Previous WSNs attempt to harvest energy from various sources, and some also use supercapacitors instead of batteries to address the battery aging problem. However, they either waste much available energy due to impedance mismatch, or they require active digital control that incurs overhead, or they work with only one specific type of source. AmbiMax addresses these problems by first performing maximum power point tracking (MPPT) autonomously, and then charges supercapacitors at maximum efficiency. Furthermore, AmbiMax is modular and enables composition of multiple energy harvesting sources including solar, wind, thermal, and vibration, each with a different optimal size. Experimental results on a real WSN platform, Eco, show that AmbiMax successfully manages multiple power sources simultaneously and autonomously at several times the efficiency of the current state-of-the-art for WSNs.

I. INTRODUCTION

Energy supply has been the greatest limiting factor on wireless sensor networks (WSN) to date. Batteries today can power a sensor node for only a few hours at 100% duty cycle, and as a result, many WSN problems have been posed to perform sporadic event detection or very low rate data acquisition to minimize the duty cycle. Unfortunately these techniques are not applicable to problems that require more computation, longer transmission distance, higher data rate, or other power consuming tasks. At the same time, many sensing environments provide sufficient energy in the form of sunlight, wind, vibration, and even water flow that can be harvested for powering the sensor nodes indefinitely. This has motivated researchers to design energy harvesting capabilities in their sensing systems. The issues are harvesting *efficiency*, *autonomy* of harvesting control, and *expandability* to multiple sources.

High harvesting efficiency is important, because it directly affects the cost and form factor of the sensing system as well as the operating lifetime. Unfortunately,

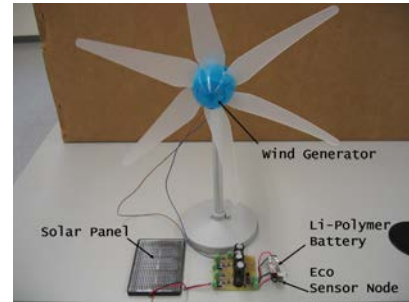


Fig. 1. Photo of AmbiMax Hardware with a Solar Panel, Wind Generator, Lithium Polymer Battery and Eco Node

most wireless sensing systems constructed to date do not extract power efficiently. As a result, they must use a much larger solar panel than necessary to yield the same level of power as a more efficient one, or they rely on a larger, more expensive, higher capacity battery than needed in order to sustain extended operation. In both cases, the low harvesting efficiency limits the achievable performance or size and can preclude the system from many important applications.

One problem that must be solved in harvesting efficiency is *maximum power point tracking* (MPPT), or impedance matching between the supply and the source at runtime. The impedance of a solar panel is primarily a function of the sunlight intensity and the current, and to a lesser extent of temperature and other factors. The maximum power point (MPP) is the point on the I-V curve that maximizes the power output at the given level of light intensity. MPPT entails sensing the relevant supply condition and setting the current limit accordingly. MPPT is applicable to not only solar panels but wind generators and virtually all other ambient power sources as well. Because of the wide dynamic range of these ambient sources, the harvesting efficiency can easily drop by one to two orders of magnitude if MPPT is not performed.

Methods for MPPT have been proposed for not only

solar panels but also for wind generator [1], [2], [3]. However, these methods are originally developed for relatively large, complex system such as satellites or industrial instruments. They rely on DSP based systems to run MPPT algorithms and can be prohibitive on small, low-power WSNs. For WSNs, researchers proposed running MPPT as a low duty task on the same microcontroller (MCU) that also performs the sensing control and power management functions. This works well if the supply condition does not change abruptly, so that MPPT need not be performed frequently relative to the application's duty cycle. However, it takes up precious I/O resources such as ADC inputs, GPIO pins or DAC pins for control, and it does not work when the MCU is asleep. For these reasons, an autonomous MPPT solution is desired.

In addition to high efficiency and autonomous operation, another consideration is expandability. Because ambient power such as solar or wind is not always available at all times and at a steady level, it is necessary to buffer up the energy during unavailable times. Moreover, one may also consider drawing power from multiple sources, e.g., from both solar and wind to increase power availability. The MPPT system should be able to compose multiple harvesting power sources to form one high-efficiency energy supply.

To address all these problems, we developed a simple and low cost platform called AmbiMax for maximum power point tracking and energy storage for wireless sensor nodes. It is implemented entirely with analog circuitry and operates autonomously without relying on any digital control. Our MPPT circuit consists of a PWM regulator controlled by the output signal of a sensor that tracks the supply condition. This approach is simple, low cost, highly efficient, and easy to implement with commercial off-the-shelf (COTS) components. Moreover, the same MPPT circuit can be applied to different types of ambient power sources simply by adjusting a few variable resistors. Since the battery is often the largest component in many wireless sensor nodes, higher harvesting efficiency combined with simplicity of implementation will also translate into a significant reduction in form factor, cost, and greatly expanded applications.

This paper is organized as follows. We review related work and provide a background on the problem of MPPT in WSNs. We describe an actual implementation of AmbiMax and compare harvesting efficiency with two wireless sensor platforms, Eco and Mica2. Experimental results show that our energy harvesting mechanism achieves significantly higher efficiency by performing

MPPT on multiple power sources simultaneously and autonomously.

II. RELATED WORK AND BACKGROUND

Several energy harvesting systems for wireless sensor systems have been proposed. Most of them use solar panels as their ambient power source, and they use batteries and supercapacitors for energy storage. This section reviews some of the recently proposed energy harvesting systems and shows the characteristics of the ambient power sources.

A. Energy Harvesting Systems

Energy harvesting systems can be categorized by the types of ambient power sources and the energy storage devices.

Helimote *Helicomote* [4] has a solar panel and two AA type NiMH batteries. It is an autonomous system: as the solar panel is directly connected to its battery through a diode, energy harvesting occurs when the solar panel's output voltage V_{solar} is 0.7V higher than that of the battery V_{batt} . When V_{batt} is higher than V_{solar} , even though ample power may be available on the solar panel, a wireless sensor node can still draw current from the battery. Moreover, it does not perform MPPT, which is essential to achieving high harvesting efficiency. As a result, to increase the harvesting efficiency, Helimote should have higher V_{solar} , which results in higher cost and larger volume. Also, it uses two AA type batteries whose maximum V_{batt} is at most 3.0 V. This V_{batt} results in low conversion efficiency when the WSN's switching regulator has to output a voltage higher than 3.0V.

Prometheus *Prometheus* [5] has a supercapacitor (22F) as a primary buffer, a Li-Polymer battery, and a solar panel. The solar panel first charges the supercapacitor, from which the system draws current when enough power is available on the solar panel. The system draws current from the battery only when the charge level of the primary buffer (V_{cap}) is less than a certain threshold, and it seldom draws power from the battery. This feature contributes to increasing the battery's lifetime, a known critical limiting factor on the lifetime of WSNs. Also, when the supercapacitor's terminal voltage (V_{cap}) is higher than a certain threshold, it charges its Li-Polymer battery. However, in this design, because the solar panel is hardwired to the supercapacitor (i.e., $V_{solar} = V_{cap} + 0.7V$), V_{cap} always follows V_{solar} when $V_{solar} > V_{cap} + 0.7V$. When $V_{solar} < V_{cap} + 0.7V$, as with Helimote, Prometheus is not able to harvest energy from the ambient power sources. Similarly, the lack of



(a) Solar Panel with Light Sensor

(b) Wind Generator with Rotor Speed Sensor

Fig. 2. Photos of Ambient Power Sources with monitoring sensors

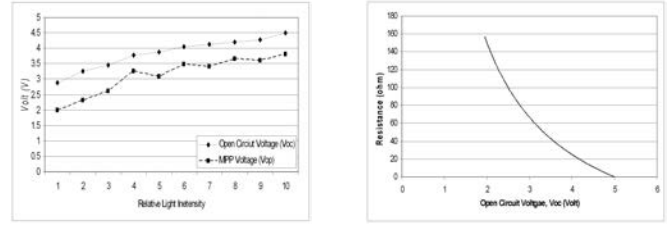
MPPT substantially limits the harvesting efficiency of Prometheus. In addition, all control tasks for energy harvesting are run on the node's microcontroller (MCU) that must perform sensing control and networking functions. It can be imposing especially for monitoring applications with hard real-time constraints.

Everlast The *Everlast* system [6] has a solar panel and a supercapacitor. It does not have a battery but does have an MPPT circuit. It charges a huge-sized supercapacitor (100F) while tracking the MPP of its solar panel. Its harvesting efficiency is much higher than Heliomote and Prometheus and does not suffer from degradation of its battery. However, its MPPT hardware requires an MCU to run the MPPT algorithm.

PUMA *PUMA* [7] is designed to maximize the utility of ambient power from a sensor system with multiple ambient power sources, leading to lower power draw from the battery. The PUMA technique uses a power routing switch to route multiple power sources to multiple subsystems. The higher utility of ambient power is achieved through a combination of MPPT and power defragmentation. However, it requires MCU control based on input from light or wind sensors.

B. Ambient Energy Sources

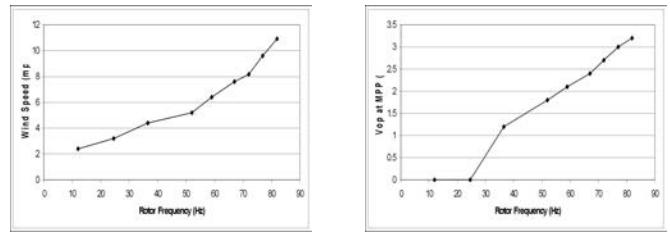
Many different types of ambient power sources have been proposed, such as vibration-to-electricity converter and thermal difference-to-electricity converter. However, the overwhelming majority of wireless nodes to date use solar panels and wind generators, because these sources deliver sufficient power for most of today's sensor nodes, which can consume up to several hundred mW. Also, these two types of power sources have been characterized extensively in the literature [1], [2], [3], [8], [9], [10], [11], [12], [13]. This paper also characterizes a solar panel and a wind generator that are used in our AmbiMax platform, although we focus primarily on those useful



(a) V_{oc} vs. Sunlight Intensity and V_{op} vs. Sunlight Intensity

(b) V_{oc} vs. Photo-Resistor Value

Fig. 3. Characteristics of Solar Panel



(a) Wind Speed vs. Rotor's Rotating Frequency

(b) V_{op} vs. Rotor's Rotating Frequency

Fig. 4. Characteristics of Wind Generator

and essential characteristics relevant to the AmbiMax system design.

Solar Panel In addition to the well known Current-Voltage and Power-Voltage characteristics [8], solar panels have another interesting property, where the open circuit voltage (V_{oc}) is near linearly proportional to the voltage at MPP (V_{op}) [12], [9], as shown in Fig. 3(a). Also, Fig. 3(b) shows that the resistance value (R_{photo}) of a light sensor (S1087 [14]) is near inversely proportional to V_{oc} . Therefore, R_{photo} can be said to be near inversely proportional to V_{op} . This fact enables the MPP to be found by measuring only R_{photo} . We use this characteristic to design a simple yet accurate MPP tracker. Design details will be presented in a later section.

Wind Generator Fig. 4(a) shows the relationship between the wind speed and the rotating frequency of a rotor. Also, Fig. 4(b) shows that the rotor frequency is near linearly proportional to V_{op} of the wind generator we used (Wind Lab, [15]). We used this fact to design the MPPT for the wind generator. We feed the rotor's frequency to V/F converter (TC9401 [16]), which outputs the proper voltage signal.

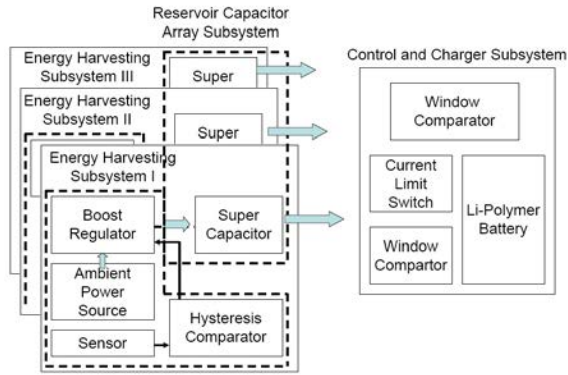


Fig. 5. Architecture of AmbiMax Platform

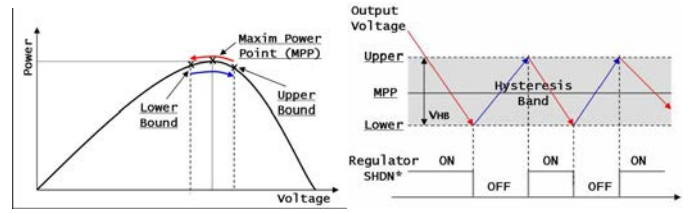
III. OVERVIEW AND PRINCIPLES OF OPERATION

Fig. 5 shows the hardware architecture of the AmbiMax platform. It consists of three subsystems: Energy Harvesting (EH), Reservoir Capacitor Array (RCA), and Control/Charger (CC). Each energy harvesting subsystem harvests energy and charges its own *reservoir capacitors* (RCs) at the source's own maximum power point. The RCs of different sources comprise the Reservoir Capacitor Array.

The system can be powered by the ambient sources or the battery. It is powered solely by the ambient sources when the RCA has a higher voltage at its terminal than a certain threshold. It draws power from the battery when the RCA's terminal voltage drops below the threshold. Eventually, the RCA's terminal voltage rises again. When the ambient power sources can generate more energy than needed to drive the system, then they also charge the battery. In AmbiMax, all of the above activities are autonomously controlled by purely analog circuitry, without the use of a digital controller. AmbiMax is also expandable to additional harvesting sources, simply by connecting their reservoir capacitor to the RCA. This section explains the principles of operation for each subsystem and discusses trade-offs for system-level optimization of these wireless sensor platforms.

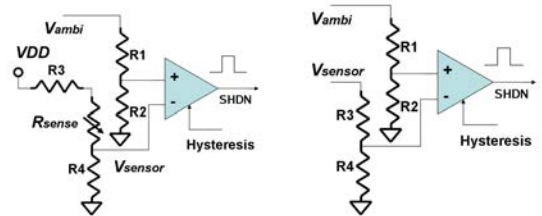
A. Energy Harvesting Subsystem

As shown in Fig. 5, the EH subsystem consists of a set of energy harvesting units, and each unit includes an ambient power source, a PWM switching regulator, and MPPT circuitry. In the ensuing text, V_{oc} , V_{ambi} and V_{op} denote the *open circuit voltage*, *short circuit voltage*, and *operating voltage at MPP* of an ambient power source,



(a) Power-Voltage Characteristics of Ambient Power Sources and Maximum Power Window (b) Hysteresis Band and Regulator's Status

Fig. 6. Maximum Power Point Tracking using a switching regulator and comparator



(a) Comparator Config. with Resistive Sensors (b) Comparator Config. with Voltage Output Sensors

Fig. 7. Comparator Configurations of MPP Tracker

respectively. Also, V_{cap} denotes the *terminal voltage* of a reservoir capacitor.

1) *PWM Switching Regulator*: In contrast to previous designs that connect the solar panel either directly to a supercapacitor or battery through a diode [5], [4], we put the PWM switching regulator between the ambient power source and the reservoir capacitors. This improves the harvesting efficiency over previous designs. First, this regulator prevents the supercapacitor from degrading the operation efficiency of the ambient power source. This isolation enables energy harvesting to continue even when $V_{oc} < V_{cap}$, a condition that causes both the Helimote and Prometheus to stop harvesting, as discussed in related work. As a result, AmbiMax can harvest energy at all times except only when the battery is fully charged and the sensor node is turned off, so that it does not consume energy. The PWM regulator also serves the purpose of a diode to block the reverse current flow from the supercapacitor to ambient power source, but without the overhead of normal 0.7V drop.

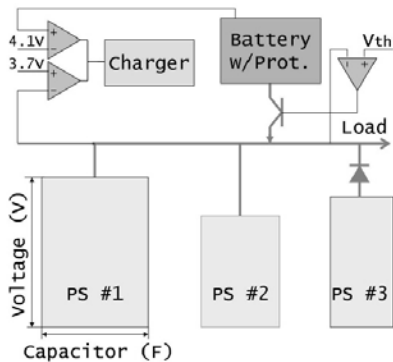


Fig. 8. Reservoir Capacitor Array

2) *MPPT Circuitry*: An ordinary PWM switching regulator by itself cannot perform MPPT when it charges a capacitor [6]. However, a switching regulator with a comparator can be used to perform MPPT, if the comparator controls the operation of a switching regulator by comparing V_{ambi} and an output signal of a sensing device (V_{sensor}), which can be generated based on the status of ambient power sources. Once V_{ambi} drops below $V_{sensor} - V_{Hysteresis}$, which means the ambient power source is out of the maximum power point, the comparator turns off the regulator. Also, when V_{ambi} increases so that it is higher than $V_{sensor} + V_{Hysteresis}$, the comparator turns on the regulator again. Fig. 6 summarizes how MPPT works on the AmbiMax platform. Previous work used an MCU to sample the source status and generate the control signal, but this will not work if the MCU must sleep. AmbiMax uses sensing devices to autonomously monitor the status of ambient power sources without digital control. For solar panels, a light intensity sensor such as a resistive sensor (S1087 [14]) or voltage output sensor (TSL250RD [17]) can be used to control on/off status of the switching regulator. The configurations of the comparator and sensing devices are described in Fig. 7. As shown in the related work section, both the sunlight intensity and the sensor's output signal are nearly linearly proportional to V_{op} . Therefore, it is definitely possible to exactly monitor the MPP of the power source by scaling both (V_{ambi}) and (V_{sensor}) using $R1 \sim R4$. For other types of ambient power sources such as a wind generator and vibration-to-electricity converter, we can use a frequency-to-voltage (FV) converter [16] and accelerometer [18], respectively.

B. Reservoir Capacitor Array

As shown in Fig. 8, the reservoir capacitors (RCs) from different energy harvesting subsystems form a

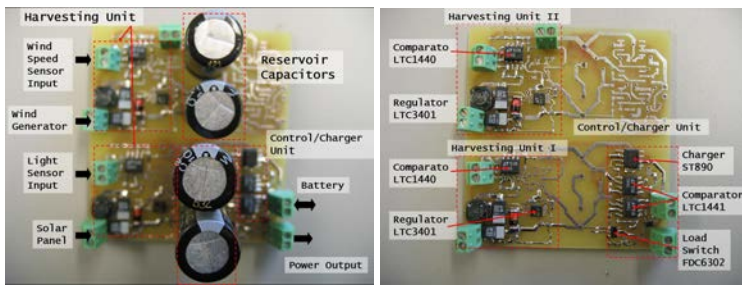
reservoir capacitor array (RCA). The RCs serve the purposes of resolving the imbalance between power generation and consumption. They smooth out the wide dynamic range and possible sudden, unpredictable change of the ambient power source, which can cause the system to operate unreliably or fail. The wide dynamic range also makes it hard to directly charge a lithium-polymer battery. They also enable preferentially drawing power from the capacitors instead of the battery whenever possible as a way to slow down battery aging due to deep discharging cycles. An RC is connected to the RCA via a diode, which has a voltage drop but provides the necessary isolation among the supercapacitors and the battery.

Each supercapacitor of this network can have a different capacity. When choosing the capacity, we should consider the characteristics of the power source as well as power consumption rate of the load system. The supercapacitor for the ambient power source with a low power output should have a smaller capacity. Otherwise, this capacitor will never deliver any current, because its terminal voltage is always lower than the other supercapacitors in the network.

C. Control and Charger

As shown in Fig. 8, the Control and Charger (CC) subsystem includes a window comparator, threshold detector, load switch, battery charger, and battery protector. This subsystem determines which power source, that is either the battery or RCA, should power the load by comparing the terminal voltage of RCA (V_{cap}) and user-configured threshold voltage V_{th} . When $V_{cap} > V_{th}$, the RCA powers the load system. Otherwise, the threshold detector turns on the load switch so that the battery powers the system. Also, the window comparator, which takes V_{cap} and $V_{battery}$, decides if the RCA charges the battery or not. When V_{cap} is higher than the threshold voltage (V_{th1}) and $V_{battery}$ is not fully charged, this comparator turns on the charger.

We use an adjustable current limit switch as the battery charger instead of COTS battery charging ICs. We reviewed different types of battery charging ICs, which may use constant current, constant voltage, linear, switching, and pulse charging, but these ICs themselves consume nontrivial power. The current limit switch allows only programmed current level to pass through the switch when it turns on. In other words, it behaves exactly the same as what the battery charger does in constant-current mode.



(a) AmbiMax Board w/ Super-capacitors

(b) AmbiMax Board w/o Super-capacitors

Fig. 9. Photo of AmbiMax Board which measures 32 mm x 24 mm

TABLE I

WSN POWER REQUIREMENTS AND ENERGY AVAILABILITY ON VINCENT THOMAS BRIDGE

WSN	Lifetime > 1 year Power Consumption < 200 mW Regulator: Switching or Linear, 3~4V output Battery: One cell Li-Ion/Polymer or Two AA type
Sunlight	at least 6 hours a day, higher than 800 Lumens
Wind	avg. 10 mps at least 6 hours

IV. IMPLEMENTATION

Fig. 9 shows the AmbiMax energy harvesting platform. Its harvesting units are connected to a solar panel and a wind generator. AmbiMax charges a Li-Polymer battery when possible, and we connect the power output terminals to power an Eco wireless sensor node [19]. This section describes the implementation details of the AmbiMax platform and addresses several trade-offs on selecting components to satisfy our design specifications.

A. Ambient Power Sources

We used Solar World's solar cell module (4-40-100) [15] whose maximum output voltage and current are 4.0V and 100mA, respectively. Also, we chose Joiniff's wind generator (Windlab Junior) [20], which can generate 500mW maximum at 2000 rpm. When we choose ambient power sources, specifically based on their output power levels, we should consider several design parameters of WSN such as expected lifetime, power consumption level, and the type and characteristics of the regulator and battery. These parameters should be matched with the availability of ambient energy at the deployment site.

Table I shows the specification of energy consumption by our WSN platform and the energy availability near *Vincent Thomas Bridge* in San Pedro, California [21].

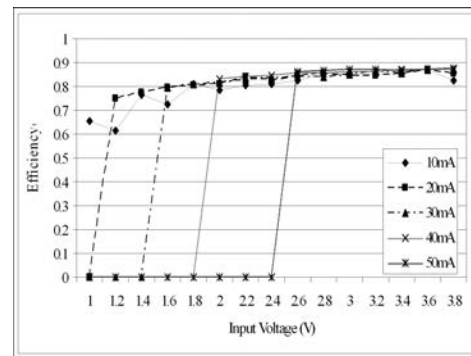


Fig. 10. Measured conversion efficiency of LTC3401 at $V_{out} = 4.1V$

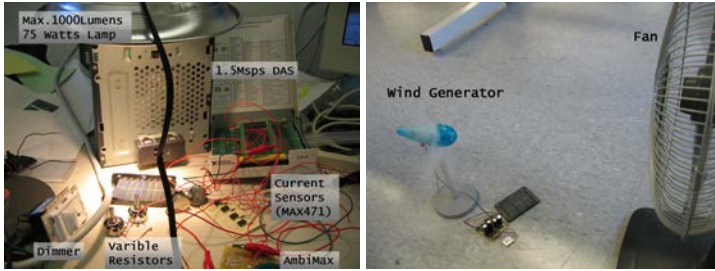
Based on the estimated local conditions, our solar panel and wind generator are expected to generate 400mW at the peak, and 200mW for at least 6 hours a day.

B. Energy Harvesting Unit

The energy harvesting unit consists of a switching regulator and an MPP tracker. The switching regulator controlled by the MPP tracker charges the supercapacitors of the RCA. We chose a boost switching regulator, the LTC3401 [22], which has a wide input voltage range of 0.5V – 5.5V, and which has high conversion efficiency over AmbiMax's operating power range. As show in Fig. 10, the conversion efficiency of LTC3401 is over 85% in the 10–50mA output current range, when its output voltage is set to 4.1V. The input voltage and current ranges are well matched with the power characteristics of our ambient power sources. The reason we set the output voltage to 4.1V is to provide the similar input voltage range (2.7V – 4.2V) to sensor nodes that are designed to use a single cell Li-Polymer or two AA type batteries. The hysteresis band of the comparator is set to 100mV, and we used very accurate 0.1% resistors for all configuration resistors, $R1 - R4$. As source sensor, we use a photodiode (S1087 [14]) and voltage-and-frequency converter (TC9401 [16]) for the solar panel and wind generator, respectively.

C. Reservoir Capacitor Array

For the reservoir capacitors, we use supercapacitors from Panasonic [23]. We connect two 22F supercapacitors in series for the solar panel, and two 10F supercapacitor in series for the wind generator. The maximum voltage of each supercapacitor is 2.3V. Because the output voltage of the harvesting regulator is set to 4.1V, we had to connect two capacitors in series to increase the voltage level. We use a high-conductance, fast diode, the 1N4148 [24].



(a) Experimental Setup for Solar Energy (b) Experimental Setup for Wind Energy

Fig. 11. Experimental Setup for AmbiMax

D. Control and Charger Unit

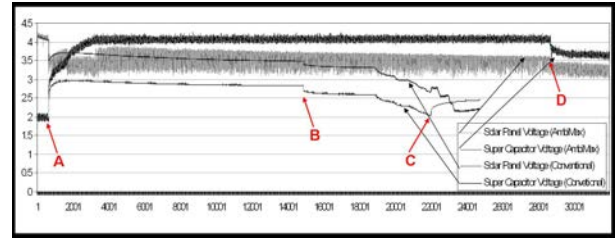
To implement the control and charger unit, we use two window comparators (LTC1441 [25]) and an adjustable current limit switch (ST890 [26]). The V_{th} is set to 2.7V so that when V_{cap} is lower than V_{th} , the battery powers the load system. We choose 2.7V because the conversion efficiency of Eco’s switching regulator [27] drops sharply under 2.7V. It is desirable to maintain the output voltage of AmbiMax higher than 2.7V to achieve high overall energy conversion efficiency. For different wireless sensor nodes and regulators, we can adjust V_{th} accordingly. Also, we set V_{th1} to 3.7V so that when V_{cap} is higher than 3.7V, AmbiMax starts to charge the battery until either V_{th1} drops below V_{cap} or the battery is fully charged.

V. EVALUATION

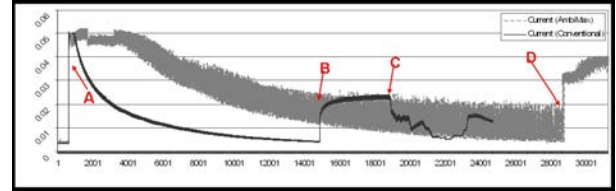
In this section, we evaluate our AmbiMax platform in terms of harvesting efficiency and overhead caused by analog control circuitry. Also, we compare our design with previous work.

A. Experimental Setup

Fig. 11 shows the experimental setup we used to evaluate the AmbiMax platform. To emulate sunlight indoors, we used a halogen lamp whose maximum light output is 1000 lumens. We vary the light output using a dimmer. To evaluate a wind energy harvesting system, we used a fan that can generate wind at a maximum speed of 16 km/h. Also, we used a data acquisition system (NI PCIe-6259 [28]) from National Instruments. To measure the current level, we used an accurate current sensor IC (MAX471 [29]). For efficiency comparison, we also implemented the harvesting system in Prometheus [5]. In that design, the solar panel is directly connected to the



(a) V_{solar} and V_{cap} of AmbiMax vs. Prometheus



(b) I_{solar} of AmbiMax vs. Prometheus

Fig. 12. Solar Energy Harvesting Efficiency Comparison During 8.8 minutes: AmbiMax vs. Prometheus. (A) Start charging the supercapacitor. (B) Connect 100Ω resistor to discharge (Prometheus). (C) V_{solar} is lower than V_{cap} . (D) Connect 100Ω resistor to discharge (AmbiMax)

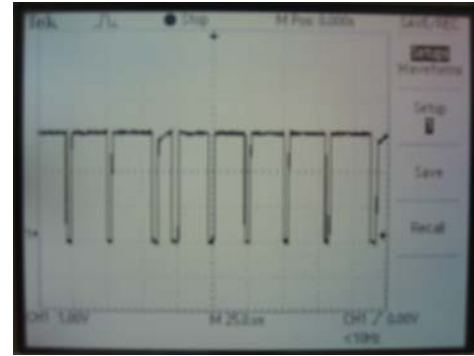


Fig. 13. Shut-Down signal from the comparator is turning on and off the harvesting regulator continuously to track MPP

supercapacitor, called the *primary buffer*. The authors did not mention if there is a diode in between the supercapacitor and solar panel, but we included a diode (1N4148) to protect the solar panel from reverse current flow.

B. Solar Harvesting Efficiency

To evaluate the solar energy harvesting efficiency, we conducted two experiments. First, we charged a 1.5F, 5V supercapacitor, which had already been charged to 2.0V, using AmbiMax. This experiment is useful to show how AmbiMax is tracking the MPP and harvesting energy

independently from the charging voltage of the supercapacitor. After the supercapacitor is fully charged up to the output voltage level of the harvesting regulator (4.1V), we did the second experiment. We connected a 100Ω resistor at the output terminal of the supercapacitor to observe how AmbiMax reacts to sudden and high current draw from the load system. During this experiment, we kept monitoring the terminal voltage (V_{solar}) and current (I_{solar}) of the solar panel and the supercapacitor's terminal voltage (V_{cap}).

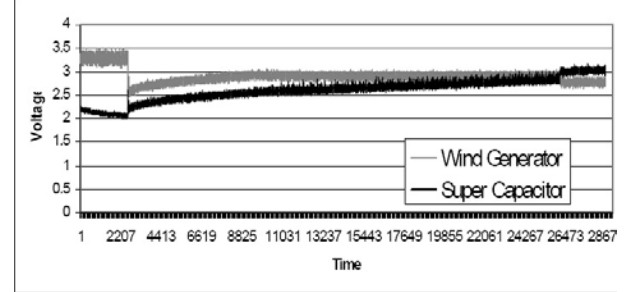
Fig. 12 shows the current and voltage profile we collected from these experiments. In Fig. 12(a), the thick gray and black lines represent V_{solar} and V_{cap} , respectively; in Fig. 12(b), the thick gray line is for I_{solar} . These two figures show that our AmbiMax platform harvests energy from the solar panel satisfying two design goals mentioned earlier. The first is the maximum power point tracking. According to Fig. 3, V_{op} (short circuit voltage at MPP) is approximately 3.5V when the V_{oc} (open circuit voltage) in this experiment is 4.05V. We can observe that V_{solar} is always swinging around 3.5V. Also Fig. 13 shows the SHDN (shutdown) signal from the comparator turning on/off the regulator to tracking the MPP. The reason for the gradual, slight drop of the output voltage over time is that the rising temperature of the solar panel causes degradation in solar panel's conversion efficiency. Also, AmbiMax continues harvesting energy even when V_{cap} is higher than V_{solar} .

For comparison, we conducted the same experiments using the harvesting system proposed for Prometheus. In Fig. 12(a) two thin lines represent V_{solar} and V_{cap} in Prometheus and other conventional designs. We can observe that their maximum V_{cap} is limited by V_{solar} . Also, when $V_{solar} > V_{cap}$, there is always a voltage gap between their V_{solar} and V_{cap} , which is caused by the diode and is non-negligible in many low-power WSNs. Therefore, under the exactly same light intensity, Prometheus's V_{cap} is always less than 3.0V, and in fact it drops further as the solar panel's terminal voltage decreases. Note that AmbiMax maintains the V_{cap} at 4.1V until it starts to discharge. Fig. 12(b), which plots I_{solar} over time, shows that the amount of current harvested by Prometheus (thin black line) to be much lower than that of AmbiMax (thick gray line) most of the time.

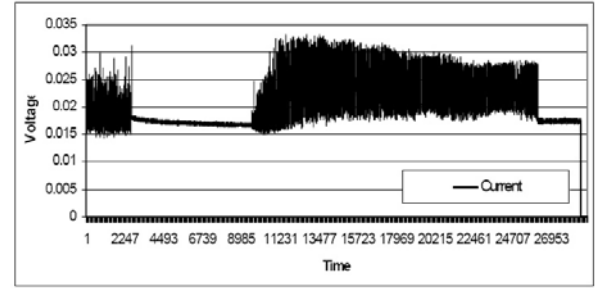
For quantitative comparison, we measure the time for V_{cap} to reach 3.0V and harvest energy during the first 20 seconds after starting to charge the supercapacitor. Table II shows that AmbiMax can charge the supercapacitor 12.5 times faster and can harvest three times more energy under identical sunlight intensity. Actually, AmbiMax is

TABLE II
HARVESTING EFFICIENCY COMPARISON

	Time	Energy
AmbiMax	0.4 secs	1318.3 J
Prometheus	5 secs	433.8 J



(a) V_{wind} and V_{cap} of AmbiMax



(b) I_{solar} of AmbiMax

Fig. 14. Wind Harvesting Efficiency Comparison During 5.2 minutes

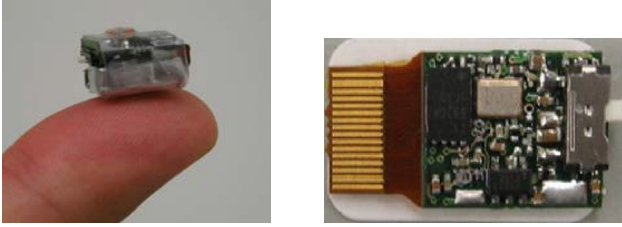
even more efficient because it can continue harvesting energy when $V_{solar} < V_{cap}$ but Prometheus cannot.

C. Wind Power Harvesting

Fig. 14 shows the power profile for AmbiMax charging the 1.5F 5V supercapacitor using a wind generator. We set the speed of the fan at approximately 8.3 meters/s and connect the supercapacitor to AmbiMax. According to Fig. 4, the MPP is about 2.7V at this speed. Fig. 14 shows AmbiMax tracking the MPP by limiting the current draw at 17–18 mA, even though the supercapacitor demands much more current.

D. Overhead

We measured the current consumed by AmbiMax's analog control circuitry and switching regulator. When we supply 3.3V to AmbiMax, it consumes less than 500 μ A.



(a) Eco Wireless Sensor Node

(b) Top View

Fig. 15. Photos of Eco Wireless Sensor Node

VI. CASE STUDY: ECO

In this section, we report the experimental result of AmbiMax over a 14-hour period. We used Eco wireless sensor node [19] for this experiment. Our experiment was conducted near the Vincent Thomas Bridge in San Pedro, CA [21] from 9:00 am to 11:00 pm. We used exactly the same hardware configuration as shown in Fig. 1. We used a 70mAh Li-Polymer battery and two 10F supercapacitors for each ambient power source. We first review the specifications of Eco and show the data from our experiments.

A. The Eco Wireless Sensor Node

Fig. 15 shows Eco wireless sensor nodes. It has a 2.4GHz radio and an 8051 compatible MCU core in the same package. The entire sensor node including the battery measures only $13 \times 10 \times 8$ mm. It consumes 22mA in receive mode and 29mA in transmit mode (at 1 Mbps and 0dBm power). We programmed the Eco node to keep sending 10 bytes of data every 1ms.

B. Experimental Data

Fig. 16 shows the experimental data collected over 14 hours. We record the terminal voltage of each of the power sources: a solar panel (V_{solar}), wind generator (V_{wind}), and battery (V_{batt}). We also record the supercapacitors' terminal voltages, V_{c_solar} and V_{c_wind} . Before the experiment starts, we charge the battery and supercapacitors until their output voltages reach 3.7V. After the experiment starts and before T_1 , the solar panel supplies power to Eco and charges the battery, because the RCA's terminal voltage, $\max(V_{c_solar}, V_{c_wind})$ is higher than the threshold (3.4V). The battery is fully charged at T_1 . From T_1 to T_3 , the solar panel powers only the Eco node, so that V_{c_solar} remains constant at 4.1V. Even though the sunlight intensity increases during this time interval, because of the thermal degradation of the solar cells,

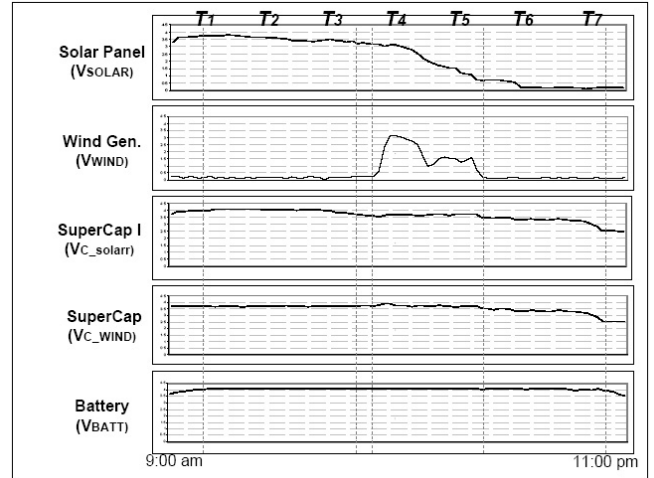


Fig. 16. 14 Hours of Experimental Data of AmbiMax platform driving Eco Sensor Node

V_{solar} decreases. At T_3 , V_{c_solar} is equal to V_{c_wind} , and during $T_3 \sim T_4$, the two supercapacitors jointly power the Eco node. At T_4 , the wind generator starts operating and charging its supercapacitor. At T_5 , all ambient power sources stop generating power, and Eco starts consuming energy stored in the two supercapacitors. During $T_5 \sim T_7$, the discharging curves of V_{c_wind} and V_{c_solar} are almost identical, because they power Eco together. At T_7 , the terminal voltage of the RCA network reaches 2.5V, causing the system to start drawing power from the battery. After T_7 , only the battery powers the Eco sensor node.

VII. CONCLUSION

We have reported the design details of AmbiMax as an energy harvesting platform for wireless sensor nodes. AmbiMax autonomously and simultaneously harvests energy from multiple ambient power sources while performing MPPT on each power source. We showed that AmbiMax can harvest three times more energy 12.5 times faster under good supply (solar, wind) condition, and can continue harvesting even at lower supply levels where previous techniques turn off. Because it uses entirely analog control without involving a microcontroller, it does not use up precious I/O pins or ADC/DAC channels and does not incur software or memory overhead. In addition to platform independence, AmbiMax's modular structure is also easily expandable to more energy harvesting sources (e.g., water flow, vibration, ...). All of these advantages, coupled with the low cost, low hardware complexity, are expected to make our AmbiMax technique readily adaptable to a wide

variety of wireless sensing applications and sustain their prolonged operation in a robust way.

ACKNOWLEDGMENTS

The authors thank Dr. Masanobu Shinozuka for his support, including experiments on the Vincent Thomas Bridge. This work was supported in part by the National Science Foundation (NSF) NSF CAREER Award CNS-0448668 and by NSF CMS-0509018.

REFERENCES

- [1] D. Corbus, I. Baring-Gould, S. Drouilhet, V. Gervorgian, T. Jimenez, C. Newcomb, and L. Flowers. Small wind turbine testing and applications development. *Windpower'99*, June 1999.
- [2] S. Islam. Maximum power point tracking of wind turbine generators. In *Australasian Universities Power Engineering Conference, AUPEC 2005*, September 2005.
- [3] V. Gevorgian, D.A. Corbus, S. Drouilhet, and R. Holz. Modeling, testing and economic analysis of a wind-electric battery charging station. *Windpower'98*, April 1998.
- [4] V. Raghunathan, A. Kansal, J. Hsu, J. Friedman, and M. Srivastava. Design consideration for solar energy harvesting wireless embedded systems. In *IPSN 2005*, April 2005.
- [5] X. Jiang, J. Polastre, and D. Culler. Perpetual environmentally powered sensor networks. In *IPSN/SPOTS 2005*, April 2005.
- [6] F. Simjee and P. Chou. Everlast: Long-life, supercapacitor-operated wireless sensor node. In *to appear, Proc. ISLPED*, October 2006.
- [7] C. Park and P. Chou. Power Utility Maximization for Multi-Supply Systems by a Load-Matching Switch. In *ISLPED'04*, pages 168–173, August 2004.
- [8] J. Santos and F. Antunes. Maximum power point tracker for PV systems. *World Climate and Energy Event*, December 2003.
- [9] J. Enslin, M. Wolf, D. Snyman, and W. Swiegers. Integrated photovoltaic maximum power point tracking converter. *IEEE Transactions on Industrial Electronics*, 44(6):769 – 773, December 1997.
- [10] E. Koutroulis, K. Kalaitzakis, and N. Voulgaris. Development of a microcontroller-based, photovoltaic maximum power point tracking control system. *IEEE Transactions on Power Electronics*, 16(1):46 – 54, January 2001.
- [11] W. Wu, N. Pongratananuku, W. Qiu, K. Rustom, T. Kasparis, and I. Batarseh. DSP-based multiple peak power tracking for expandable power systems. In *Applied Power Electronics Conference and Exposition, 2003. APEC '03. 18th Annual IEEE*, volume 1, pages 525 – 530, 2003.
- [12] D. Lee, H. Noh, D. Hyun, and I. Choy. An improved MPPT converter using current compensation method for small scaled PV-applications. In *Applied Power Electronics Conference and Exposition, 2003. APEC '03. 8th Annual IEEE*, volume 1, pages 540 – 545, 2003.
- [13] T. Noguchi, S. Togashi, and R. Nakamoto. Short-current pulse-based maximum-power-point tracking method for multiple photovoltaic-and-converter module system. *IEEE Transactions on Industrial Electronics*, 49(1):217 – 223, February 2002.
- [14] Hamamatsu. Si photodiode S/1087/S1133 series. http://sales.hamamatsu.com/assets/pdf/parts_S/S1087_etc.pdf.
- [15] Solarworld. Solar mini-panels and motors. <http://www.solar-world.com/SolarMini-Panels&Motors.htm>.
- [16] Microchip. TC9400/9401/9402 voltage-to-frequency/frequency-to-voltage converters. <http://ww1.microchip.com/downloads/en/DeviceDoc/21483C.pdf>, 2006.
- [17] TSL250RD light-to-voltage optical sensors. <http://www.taosinc.com/images/product/document/TSL250RD-E16.pdf>.
- [18] Silicon Designs, Inc. SD1221 accelerometer. <http://www.silicondesigns.com/Pdf/1221.pdf>, 2005.
- [19] C. Park, J. Liu, and P. Chou. Eco: an ultra-compact low-power wireless sensor node for real-time motion monitoring. In *IPSN/SPOTS 05*, pages 398 – 403, April 2005.
- [20] Windlab Junior. <http://www.jointiff.com/wind.htm>.
- [21] San Pedro Peninsula Chamber of Commerce. Vincent Thomas Bridge, San Pedro, CA. <http://www.sanpedrochamber.com/champint/vtbrdg.htm>, 1996–2002.
- [22] Linear Technology. LTC3401 1A, 3MHz micropower synchronous boost converter. <http://www.linear.com/pc/downloadDocument.do?navId=H0,C1,C1003,C1042,C1031,C1060,P1897,D2673>, 2001.
- [23] Panasonic. Electric double layer capacitors (gold capacitor)/HW. <http://www.panasonic.com/industrial/components/pdf/ABC0000CE8.pdf>.
- [24] Fairchild Semiconductor. 1N4148 Diode. <http://www.fairchildsemi.com/pf/1N/1N4148.html>.
- [25] Linear Technology. LTC1440 comparator with internal reference and programmable hysteresis. <http://www.linear.com/pc/downloadDocument.do?navId=H0,C1,C1154,C1002,C1463,P1172,D2764>, 1996.
- [26] ST Microelectronics. ST890 1.2A current limited high side with thermal shutdown. <http://www.st.com/stonline/books/pdf/docs/8649.pdf>, 2005.
- [27] Linear Technology. LTC3402 2A, 3MHz micropower synchronous boost converter. <http://www.linear.com/pc/downloadDocument.do?navId=H0,C1,C1003,C1042,C1031,C1061,P1901,D2814>, 2000.
- [28] National Instruments. 16bit 1.25Msps data acquisition system. <http://sine.ni.com/nips/cds/view/plang/en/nid/201814>, 2005.
- [29] Maxim. Max471/Max472: Precision, high-side current-sense amplifiers. <http://pdfserv.maxim-ic.com/en/ds/MAX471-MAX472.pdf>, 1996.